Three-dimensional Magnetotelluric Modeling of data from Northeast of Gorgan Plain

Omid Bagherpur[1], Banafsheh Habibian Dehkordy[2*], and Behrooz Oskooi[3]

[1]*M. Sc., Department of Geophysics, Institute of Geophysics, University of Tehran, Tehran, Iran*
[2]*Assistant Professor, Department of Geophysics, Institute of Geophysics, University of Tehran, Tehran, Iran*
[3]*Associate Professor, Department of Geophysics, Institute of Geophysics, University of Tehran, Tehran, Iran*

(Received: 25 December 2017, Accepted: 24 October 2018)

Abstract

Magnetotelluric measurements have been conducted in the period range of 0.005-128 s along five parallel east-west directed profiles including 85 sites totally in the north-eastern part of Gorgan Plain, Golestan Province, North of Iran; with the aim of exploring iodine. Distortion and dimensionality analysis of data imply the existence of a north-south elongated two-dimensional model with some localized three-dimensional effects, particularly at long periods, that has been mildly affected by non-inductive distortions. Exclusion of a very few data points with large values of distortion angles and rotation based on the selected azimuth of strike was followed by two-dimensional inversion of joint TE- and TM-mode apparent resistivity and phase data. After some resolution tests to ensure the reliability of the detected features, three-dimensional inversion of real and imaginary parts of full impedance tensor data was accomplished. Despite the reduced resolution of magnetotelluric data in a conductive environment, the elimination of part of the data due to hardware constraints and the lack of an ideal data acquisition pattern, the models showed some definite results. The resulted electrical resistivity models from both two- and three-dimensional inversion resolved highly conductive bodies as our exploration targets, which are expected to be saline aquifers containing iodine within the generally conductive sediments.

Keywords: magnetotellurics; two- and three-dimensional inversion; iodine exploration; electrical conductivity

[*]Corresponding author: banafsheh_habibian@yahoo.com

1 Introduction

The study area, Dashli-Broon, is located in the westernmost part of Koppeh Dagh zone with the overall morphology of ridge-forming anticlines and valley-forming synclines, and Gorgan plain is one of the depressions. It is considered as a part of east continuation of Alborz mountain range but with different geological and structural features than adjacent areas. Sediments of the area reach a thickness of up to 10000 meters and include Mesozoic and Cenozoic sediments deposited on the Paleozoic bedrock in the northwest-southeast direction. The area has a very smooth topography ($\pm 10\ m$) and is in the form of a plain in most parts (Hollingsworth et al., 2006).

Deposits of minerals in underground brines are one of the main non-organic sources of iodine as one of least-abundant elements of the Earth. Iodine in this case is frequently found combined with sodium and potassium and in highly variable concentration. It is of oceanic origin, transferred to the atmosphere and then to the subsurface through raining.

There are various examples of the use of the magnetotelluric method in the investigation of groundwater potential and detection of aquifers and their contamination in the literature (Alies & Rodriguez, 2015; Asaue et al., 2012; Falgàs et al., 2005; Mejias et al., 2008; MeliI et al., 2011; Pedersen et al., 2005; Steuer et al., 2008). Considering that the study area is located at a proper distance from the Caspian Sea, it has the potential for geological storage of iodine reserves. The groundwater resources in the study area are most likely contain salts with a high percentage of iodine as a rare mineral.

Magnetotelluric data were acquired in 2010 and 2011 using GMS05 and MTU2000, respectively, and processed using the robust technique of Smirnov (2003) to extract the impedance tensors. The locations of the MT measurements, conducted in the range of 0.0055-128 s with the total of 85 sites are shown in Figure 1. Profiles are approximately separated with 2 km and site spacing is about 1 km.

In the previous investigation of the data, a different data-set was used; no strike angle was estimated, and resistivity models derived from one- and two-dimensional inversion of the determinant of the impedance tensor were presented (Oskooi and Mansoori, 2015). In this paper, the results of strike estimation and distortion analysis, as well as inversion of joint TE-TM mode data and three-dimensional inversion have been discussed.

The results of data analysis is presented in section 2. Then, the application of inversion procedures is described in section 3; interpretation of the resistivity models and conclusion are presented in sections 4 and 5, respectively.

2 Magnetotelluric data analysis

Magnetotellurics is a passive geophysical method in which diffusively propagating electromagnetic signals are used to infer the electrical conductivity of the subsurface in the depth range determined by the recorded frequency range. Fluctuations in the natural electromagnetic fields are measured simultaneously and the Fourier transforms of the horizontal electric (E_x, E_y) and magnetic (H_x, H_y) fields are linearly related via the impedance tensor (Z) as:

$$\begin{bmatrix} E_x \\ E_y \end{bmatrix} = \begin{bmatrix} Z_{xx} & Z_{xy} \\ Z_{yx} & Z_{yy} \end{bmatrix} \begin{bmatrix} H_x \\ H_y \end{bmatrix} \quad (1)$$

Real value apparent resistivity and phase data are calculated as:

$$\rho_{a,ij} = \frac{1}{\mu_0 \omega} \left| Z_{ij} \right|^2, \quad (2)$$

$$\varphi_{ij} = \arg\left(Z_{ij}\right), \quad (3)$$

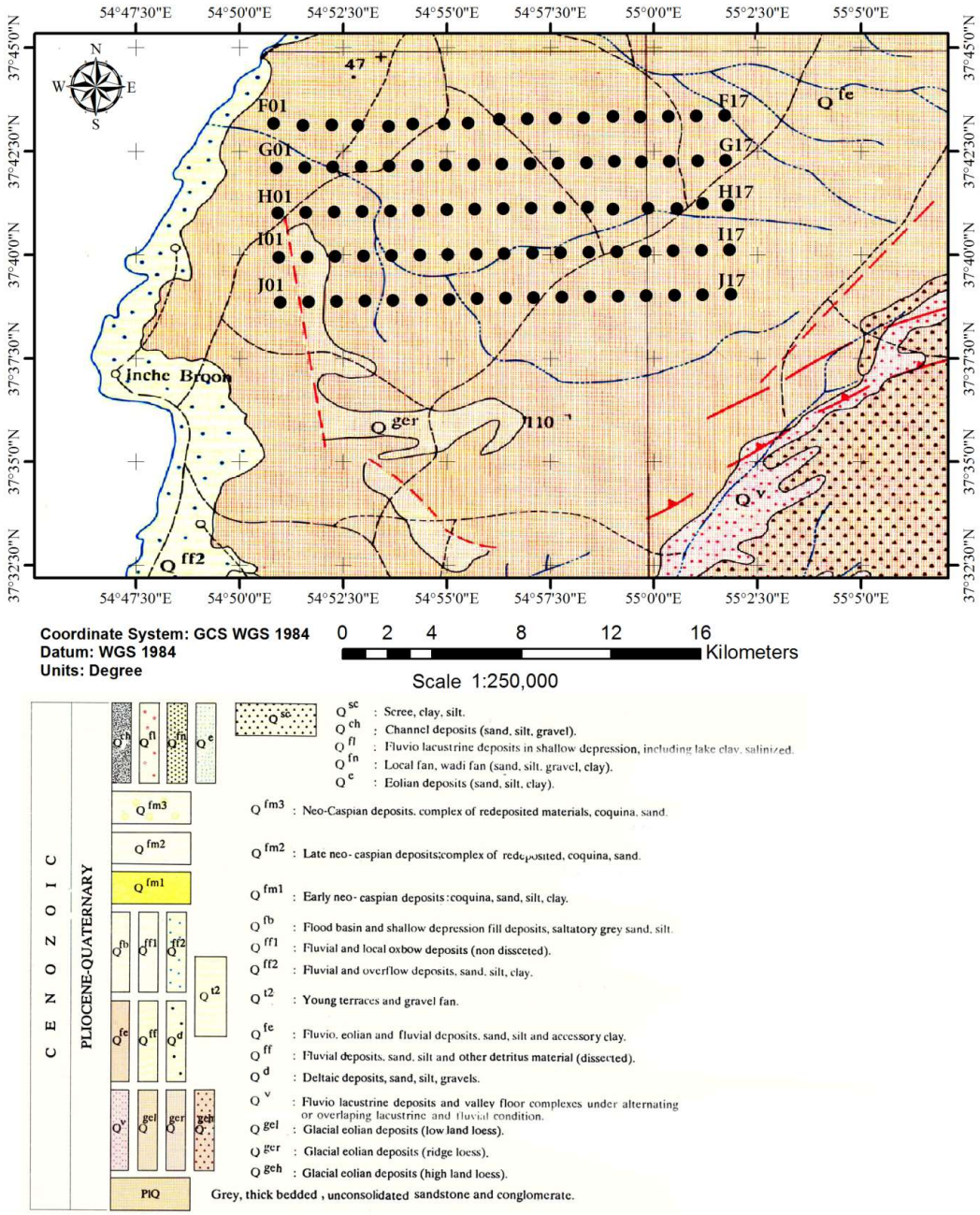

Figure 1. Geological map of the study area and distribution of MT sites. The 85 black dots are magnetotelluric stations used in this study. The study area is almost geologically uniform and covered by Quaternary fluvial deposits, sand, silt, and clay.

where ω and μ_0 are angular frequency and magnetic permeability of free space, respectively.

The strike and dimensionality of the data are estimated based on the phase tensor method (Caldwell et al., 2004). The phase tensor (Φ) is defined by the ratio of the real (X) and imaginary (Y) parts of the impedance tensor:

$$\Phi = X^{-1}Y \quad (4)$$

It is not affected by galvanic distortion of the electric field and requires no assumption of the underlying resistivity structure. Considering the phase tensor coordinate invariants, the rotational invariant phase tensor skew angle (β) is defined as the measure of the tensor's

asymmetry and can be used to evaluate dimensionality of the subsurface structures:

$$\beta = \frac{1}{2} tan^{-1}\left(\frac{\Phi_{12}-\Phi_{21}}{\Phi_{11}+\Phi_{22}}\right) \quad (5)$$

Non-zero, larger than some threshold value, skew angles are indication of the three-dimensionality. The azimuth of the geoelectric strike is determined based on the orientation of the tensor's principal axes $(\alpha - \beta)$:

$$\alpha = \frac{1}{2} tan^{-1}\left(\frac{\Phi_{12}+\Phi_{21}}{\Phi_{11}-\Phi_{22}}\right) \quad (6)$$

The results can be represented using the phase tensor ellipses. Figure 2 displays a map of phase tensor ellipses for the whole frequency range and the characteristic profile I. Similar results are obtained for other profiles. The color bar shows the skew angle values. As it can be seen, data show mainly one-dimensional behavior (low values of the skew angle) with some local two- and three-dimensional effects, especially at long periods. They are correlated with the irregular orientation of the major axes of the phase tensor ellipses and/or rounded ellipses.

The results of strike calculation based on the phase tensor method have been summarized in the rose diagrams of Figure 3. Due to the lack of lithological changes and proximity of the stations, the estimated values for the strike are expected to be similar for all profiles. In spite of the scattering in the resulting values, the azimuth of either 0 or 90° is confirmed for all profiles. This preferential direction becomes more obvious by looking at azimuths of all of the data in a single histogram.

Given that the vertical component of the magnetic field has not been measured, and so the tipper data are not available to resolve 90 degree ambiguity, based on geological information, the preferential azimuth of strike has been selected to be in the East-West direction.

The regional magnetotelluric response can be distorted due to the presence of the small-scale near-surface structures. The level of distortion was examined using WAL rotational invariants (Weaver et al., 2000) implemented in WALDIM

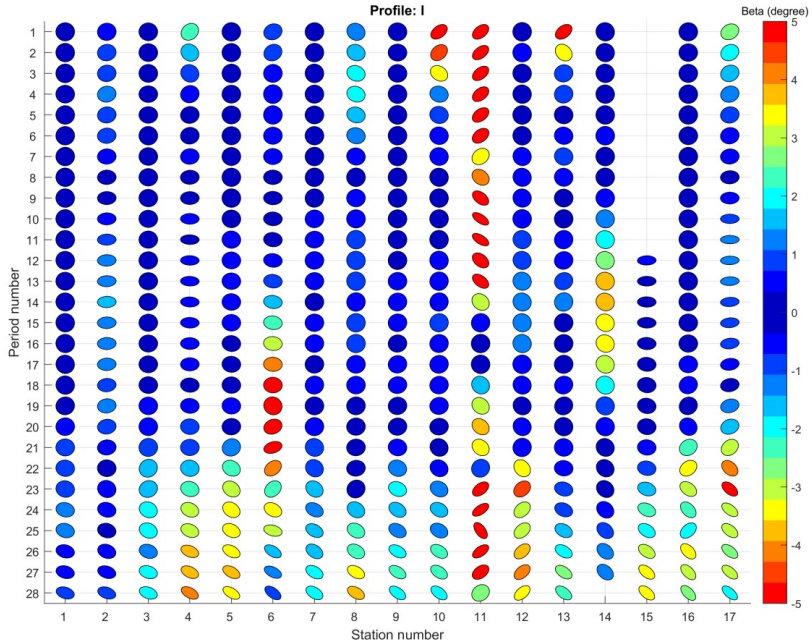

Figure 2. Map of phase tensor ellipses (28 periods and 17 sites) for the characteristic profile I.

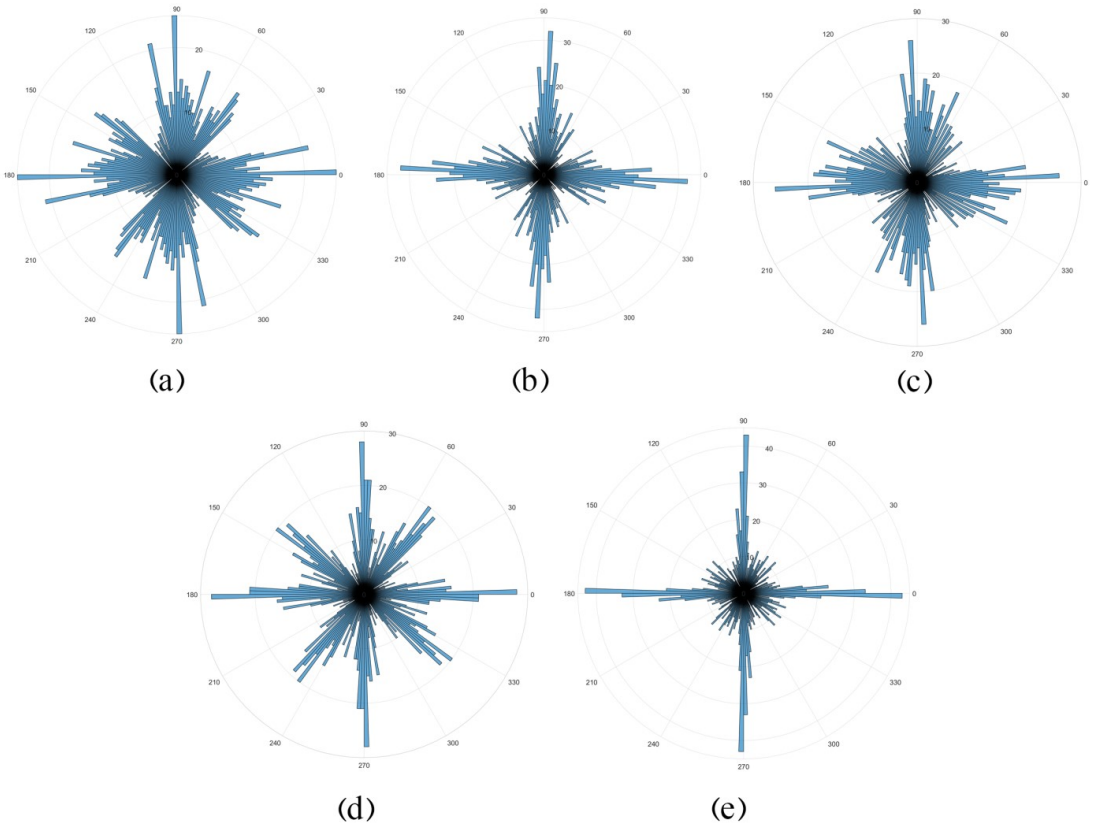

Figure 3. Rose diagrams of phase tensor strike directions for profile F (a), G (b), H (c), I (d) and J (e). The dominant directions of North-South and East-West are obvious.

code (Marti et al., 2009). Based on the values of a set of eight rotational invariants, including seven independent and a dependent parameter and considering threshold values for each of them regarding the level of present noise-dimensionality, strike direction and values of shear and twist angles as part of distortion parameters along with their errors are estimated. The galvanic distortion effects of the electric field can be described by two undeterminable parameters including static shift and anisotropy, and two determinable parameters including twist and shear angles (Groom and Bailey, 1989). Figure 4 shows the histogram of the estimated twist and shear angles for the characteristic profile I. Low values of these two parameters indicate that the data have not been severely affected by distortion.

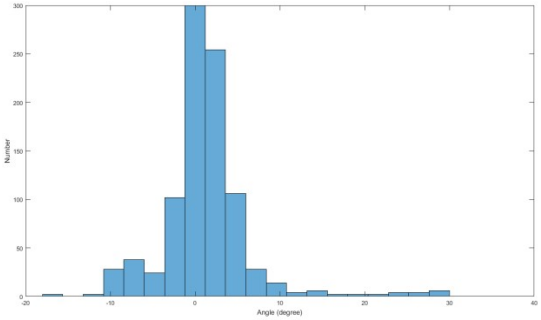

Figure 4. Histogram of the distortion parameters: twist and shear angles for characteristic profile I. more than 97% of the values lie in the range of -15 to 15 degrees, indicative of relatively small distortion.

3 Inversion Results

3.1 Two-dimensional inversion

In the case of a 2-D model, electromagnetic fields can be decoupled into transverse electric (TE) and transverse magnetic (TM) modes for which electric currents flow parallel to and perpendicular on the strike,

respectively. Apparent resistivity and phase of both TE and TM mode were selected as the input data for two-dimensional inversion. Since the inversion of magnetotelluric data is based on electromagnetic induction, the non-inductive or galvanic effects cannot be treated during this process and should be minimized. For this purpose, a very few data with twist and shear angles larger than 15° were excluded from the inversion procedure. The REBOCC code (Siripunvaraporn and Egbert, 2000), which is based on finding the smoothest model subject to an appropriate fit to the data, was applied for two-dimensional inversion. A relative error floor of 20% and an absolute error floor of 1.5 ° was set for apparent resistivities and phases, respectively. In this way, the effect of probable static shift will be reduced. However, the static shift correction was also applied. The inversion was repeated with the selection of different correction coefficients and, as expected, it was found that the data of the study area have not significantly been affected by static shift phenomena.

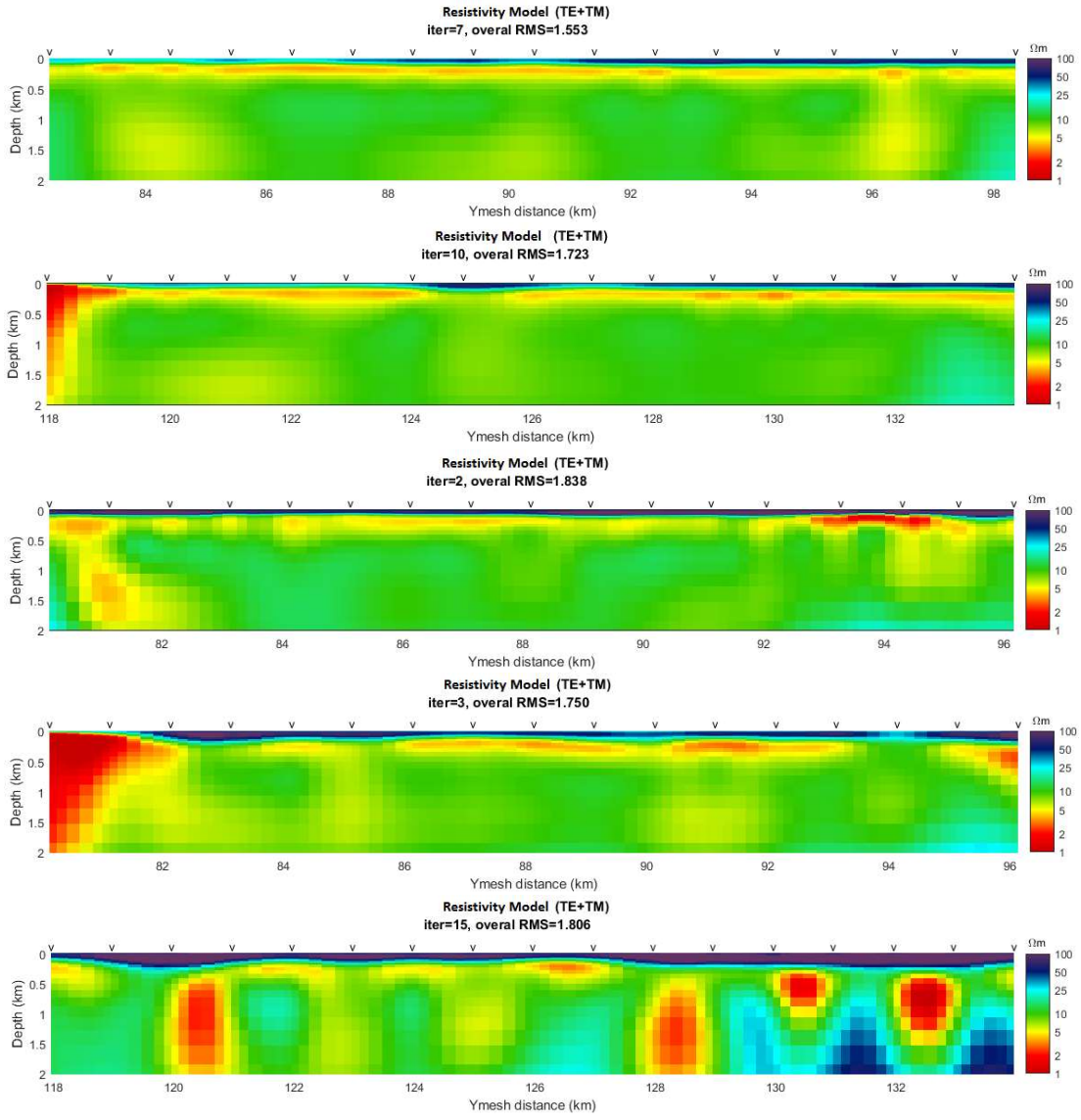

Figure 5. Two-dimensional electrical resistivity model obtained from joint inversion of TE- and TM-mode data, from top to bottom for profiles F, G, H, I and J.

The study area is covered with Quaternary sediments, and there are no specific changes of lithology. A 10 ohm.m homogeneous half-space was, therefore, chosen as the starting model for all inversions. Models resulted from the joint inversion of TE- and TM- modes for all profiles are shown in Figure 5. They were converged to RMS value of 1.43 on average. To confirm that results are real and needed for fitting of the data, sensitivity analysis was done on the main features of the model. According to the second approach noted by Juanatey et al. (2013), we performed sets of inversions for each profile data set using different prior models that were designed with maximum similarity to the final model of inversion, and only the resistivity of a considered feature varied in each inversion. This procedure aims to see how the inversion minimizes the misfit while staying close to our selected prior model. In this way, all the structures seem to be needed by the data and cannot be excluded from the final model.

3.2 Three-dimensional inversion

Sometimes it is not possible to select a single strike direction for different period intervals or for all stations. We encountered this issue for profiles F and I that show different direction for long periods. Considering this issue as well as some of the limited 3D effects observed in the region, and with the aim of obtaining an improved model, three-dimensional inversion was applied to the data. In this case, since the decomposition into two modes is erroneous, the joint fitting of the TE- and TM-mode data is difficult.

As Siripunvaraporn et al. (2005) have shown, although the most ideal data acquisition pattern of 3D inversion is an array, the 3D inversion of profile data can also provide information about off-profile structures.

The 3D inversion was accomplished using the WSINV3DMT (Siripunvaraporn et al. 2005), which inverts the full impedance tensor. The designed grid has 27, 21 and 30 cells in the north-south, east-west and vertical directions, respectively. The area covered by the stations was modeled by 1000 m × 1000 m cells and block sizes were increased by a factor of 1.2 in all directions. Full impedance tensor of 85 magnetotelluric sites in 10 equally distributed periods of 28 periods was used in the inversion. A 10 ohm.m homogenous half-space was used as the initial model and the impedance error floor was set at 5%. Three-dimensional resistivity models from two different viewing angles are shown in Figure 6. Of course, the result of the 3D inversion and the accuracy of the model have been influenced by the coarse mesh chosen due to computational constraints.

Data fitting is very similar in two- and three-dimensional inversions and in this regard, none of the models can be preferred. However, the subsequent sensitivity analyses show that, despite the remarkable similarity of the results, the 3-D is slightly more accurate in terms of positioning and conductivity imaging.

4 Interpretation of the resistivity models

The relatively low resistivity of sediments which are present in the region up to the depth of interest, has limited the penetration of electromagnetic signals. Iodine in this region is expected to be found within the saline aquifers, and thus, areas with very low resistivity in the models are of concern.

Since the goal is to identify areas with a very low resistivity, corresponding to the saline aquifers, in a general conductive area, the resistivity values less than 5 ohm.m have been isolated in Figure 7. Due to the high conductivity of the sediments, the resolution of the magnetotelluric data, which is maximum for detection of local conductors in a resistive medium, decreases.

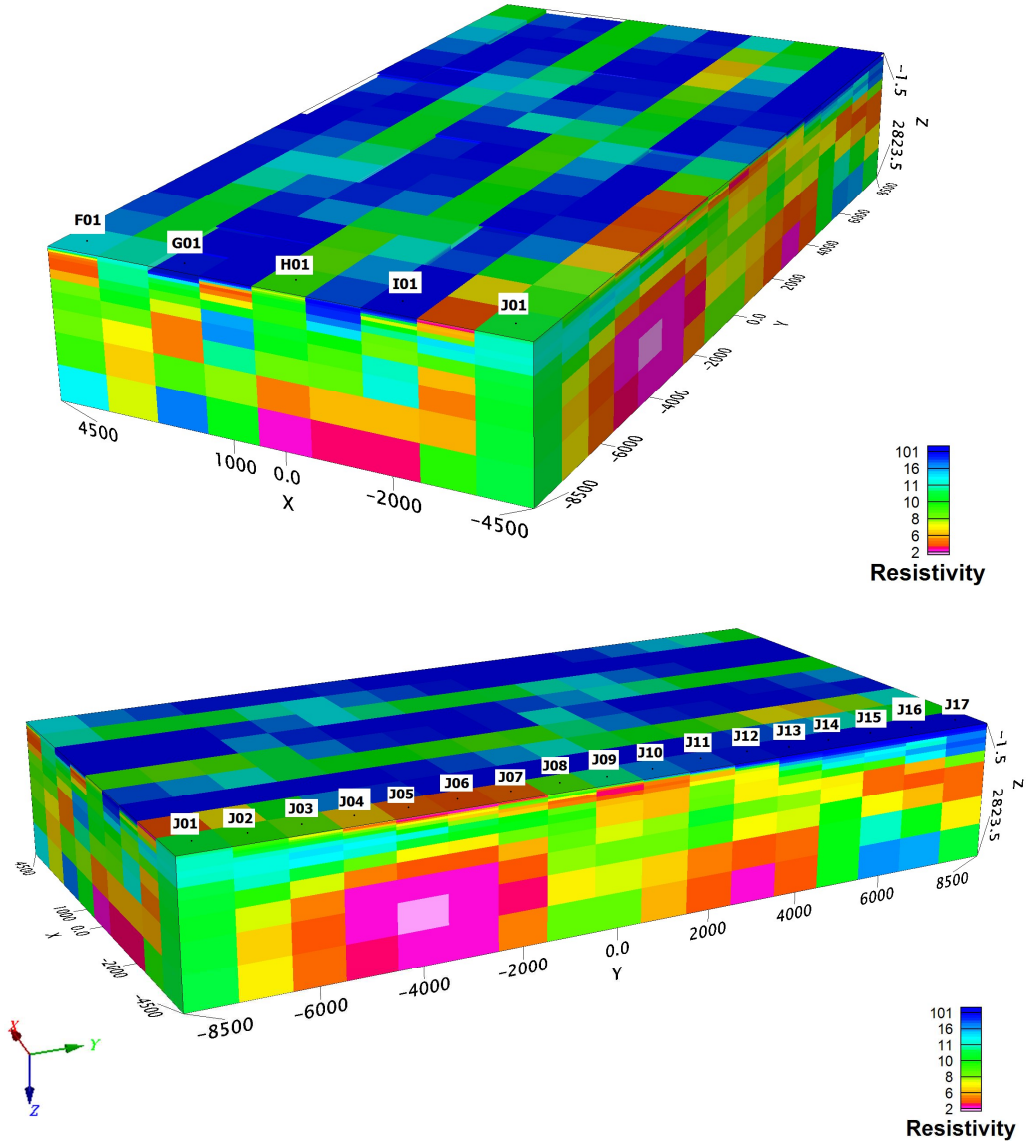

Figure 6. Three-dimensional electrical resistivity model from two different viewing angles.

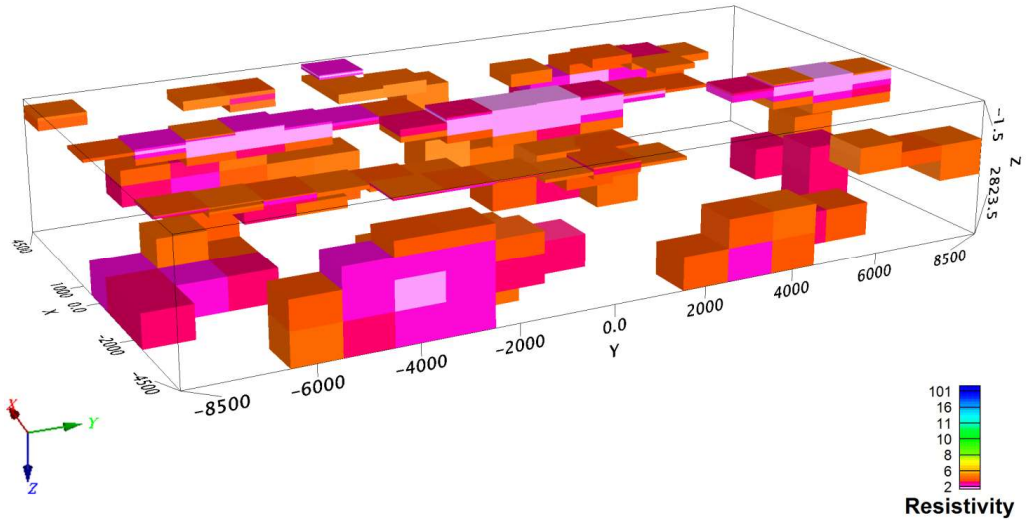

Figure 7. The corresponding volume of less than 5 ohm.m resistivity values in the final model resulted from 3D inversion.

A relatively resistive layer with resistivity values larger than 100 ohm.m has been appeared in all models resulted from both two- and three-dimensional inversions with slight differences. The thickness of this layer, which cannot be very interesting in this study, maximally reaches 100 m.

Immediately below this resistive layer, a conductive layer with variable thickness (100 m to 300 m) is observed particularly in the 2D sections of all profiles and its conductivity can be attributed to the presence of sediments in the region. This conductive layer probably contains iodine-bearing salt water. For iodine extraction; however, a larger and probably deeper storage should be sought.

There are conductive anomalies which appear more clearly and with higher conductivity in the final model of 3D inversion and are highlighted in Figure 7. The top-layer of these scattered features is estimated to be at a depth of 500 to 700 meters, and some of them extend deep to a depth of more than 2 km. Very low resistivity (less than 5 ohm.m) anomalies are suitable places for our exploratory purpose.

There is an enhanced conductivity feature at the beginning of profile G, which is common between two- and three-dimensional models and the results of sensitivity analysis confirm the very low conductivity of this structure. Therefore, drilling up to a depth of 2 km is suggested in this location. A very conductive anomaly is also observed at the end of profile H that appears with higher resolution in the 3-D model. The very low resistivity of this anomaly has been confirmed through sensitivity analysis. Therefore, this anomaly is also important to explore iodine, and the suggestion of drilling on its position seems logical.

As already mentioned, there is no expectation that iodine can be observed in high concentrations. Electrical resistivity, however, is sensitive to the presence of a small amount of conductive phase (here iodine in combination with other elements) with proper distribution and is significantly reduced. Therefore, high detected values of conductivity can be attributed to the probable presence of iodine, although not in high concentrations.

Compared to the models of this area presented by Oskooi and Mansoori (2015), the obtained models are more accurate with enhanced resolution. That is because new data has been incorporated and has reduced the site-spacing compared to the previous work, where places that have been identified as locations with high potential to be iodine reserves, are at larger depths and have more spatial scattering than our results.

Finally, some scattered conductive features were resolved in both 2-D and 3-D final models; however, the size and position of those structures might be slightly different. This might be due to the computational power limitation, which forced us to reduce the total number of data points used in the 3-D inversion, and also we had to design a much coarser mesh grid to be able to run the 3-D inversion code. On the other hand, there are some conductive structures that only showed up on either final 2-D models or the 3-D model. Meanwhile, the complexity of the structures at longer periods has been confirmed by the performed analysis of the dataset used in this paper. Consequently, a sensitivity analysis of the suspicious resolved structures at deeper depths on the 3-D model is highly suggested for future studies.

5 Conclusion

Magnetotelluric method has been used to study the subsurface electrical conductivity structure of Dashli-Broon in Golestan province, North of Iran with the

purpose of exploration of deep iodine, containing salt water. Modern data analysis methods were applied to assess the dimensionality and the level of distortion. By rotating impedance tensor to the azimuth of strike, apparent resistivity and phases of both TE and TM modes were jointly inverted. Three-dimensional inversion was also applied to possibly improve the conductivity models. Extremely low resistivity bodies, which are supposed to be salt reservoirs that probably bear iodine, were identified from the derived models and can be suggested for future drilling.

References

Ailes, C. E., and Rodriguez, B. D., 2015, Magnetotelluric data collected to characterize aquifers in the San Luis Basin, New Mexico: U. S. Geological Survey Open-File Report 2014–1248, 9 p., http://dx.doi.org/10.3133/ofr20141248.

Asaue, H., Kubo, T., Yoshinaga, T., and Koike, K., 2012, Application of magnetotelluric (MT) resistivity to imaging of regional three-dimensional geologic structures and groundwater systems: Natural Resources Research, **21**(3), 383-393.

Caldwell, T. G., Bibby, H. M., and Brown, C., 2004, The magnetotelluric phase tensor: Geophysical Journal International, **158**, 457-469.

Falgàs, E., Ledo, J., Teixidó, T., Gabàs, A., Ribera, F., Arango, C., Queralt, P., Plata, J. L., Rubio, F., Peña, J. A., Martí A., and Marcuello, A., 2005, Geophysical characterization of a Mediterranean costal aquifer, Baixa Tordera fluvial deltaic aquifer unit: Groundwater Saline Intrusion, **15**, 395-404.

Groom, R. W., and Bailey, R. C., 1989, Decomposition of magnetotelluric impedance tensor in the presence of local three-dimensional galvanic distortions: Journal of Geophysical Research, **94**, 1913-1925.

Hollingsworth, J., Jackson, J., Walker, R., Gheitanchi, M. R., and Bolourchi, M. J., 2006, Strike-slip faulting, rotation, and along-strike elongation in the Kopeh-Dagh mountains, NE Iran: Geophysical Journal International, **166**, 1161-1177.

Juanatey, M. G., Hübert, J., Tryggvason, A., and Pedersen, L. B., 2013, Imaging the Kristineberg mining area with two perpendicular magnetotelluric profiles in the Skellefte Ore District, northern Sweden: Geophysical Prosoecting, **61**, 200-219.

Marti, A., Queralt, P., and Ledo, J., 2009, WALDIM, A code for the dimensionality analysis of magnetotelluric data using the rotational invariants of the magnetotelluric tensor: Computers and Geosciences, **25,** 2295–2303.

Meji′as, M., Garcia-Orellana, J., Plata, J. L., Marina, M., Garcia-Solsona, E., Ballesteros, B., Masque, P., Lopez, J., and Fernandez-Arrojo, C., 2008, Methodology of hydrogeological characterization of deep carbonate aquifers as potential reservoirs of groundwater: Case of study, the Jurassic aquifer of El Maestrazgo (Castellón, Spain): Environmental Geology, **54**(3), 521–536.

Meli′i, J. L., Njandjock, P. N., and Gouet, D. H., 2011, Magnetotelluric method for groundwater exploration in crystalline basement complex, Cameron: Journal of Environmental Hydrology, **19**, x–y.

Oskooi, B., and Mansoori, I., 2015, Iodine-bearing saline aquifer prospecting using magnetotelluric method in Golestan plain, NE Iran: Arabian Journal of Geoscience, **8,** 5959–5969.

Pedersen, L. B., Bastani, M., and Dynesius, L., 2005, Groundwater exploration using combined controlled-source and radiomagnetotelluric techniques: Geophysics, **70**, G8-G15.

Siripunvaraporn, W., and Egbert, G., 2000, An efficient data-subspace inversion method for 2-D magnetotelluric data: Geophysics, **65** (3), 791-803.

Siripunvaraporn, W., Egbert, G., Lenbury, Y., and Uyeshima, M., 2005, Three-dimensional magnetotelluric inversion: data-space method: Physics of the Earth and Planetary Interiors, **150,** 3–14.

Siripunvaraporn, W., Egbert, G., and Uyeshima, M., 2005, Interpretation of two-dimensional magnetotelluric profile data with three-dimensional inversion, synthetic examples: Geophysical Journal International, **160,** 804–814.

Smirnov, M. Y., 2003, Magnetotelluric data processing with a robust statistical procedure having a high breakdown point: Geophysical Journal International, **152,** 1–7.

Steuer, A., Helwig, S. L. and Tezkan, B., 2008, Aquifer characterization in the Quarzazate Basin (Morocco),: A contribution by TEM and RMT data: Near Surface Geophysics, **x**, 5–14.

Weaver, J. T., Agarwal, A. K., and Lilley, F. E. M., 2000, Characterization of the magnetotelluric tensor in terms of its invariants: Geophysical Journal International, **141,** 321–336.